Racemization mechanism of lithium tert -butylphenylphosphido-borane: A kinetic insight

Rémy Fortrie, David Gatineau, Damien Hérault, Aurélie Béal, Jean-valère Naubron, Laurent Giordano, Gérard Buono

Racemization Mechanism of Lithium *tert*-Butylphenylphosphido-borane; A Kinetic Insight.

Rémy Fortrie,*[a] David Gatineau,[b] Damien Hérault,[a] Aurélie Béal,[a] Jean-Valère Naubron,[c] Laurent Giordano,[a] Gérard Buono *[a]

Abstract: The racemization mechanism of *tert*-butyl-phenylphosphido-borane is investigated experimentally and theoretically. Based on this converging approach, it is shown, first, that several phosphido-borane molecular species coexist at the time of the reaction and, second, that one particular of both initially assumed reactive routes most significantly contribute to the overall racemization process. From our converging modelling and experimental measurement, it comes out that the most probable species to be here encountered is a phosphido-borane-Li(THF)$_2$ neutral solvate, which P-stereogenic center monomolecular inversion through a Y-shaped transition structure ($\Delta_rG^{\circ\neq}$: 81 kJ.mol^{-1}) brings the largest contribution to the racemization process.

Keywords: kinetic resolution, chiral ligand, DFT modeling, kinetic modeling, complex reaction scheme analysis

Introduction

Chiral phosphines significantly contribute to the development of asymmetric processes as ligands in transition metal-catalyzed reactions[1-4] or as organo-catalysts.[5-7] The chirality of these ligands can be located on the backbone, the phosphorus atom or both. At the moment, usage of P-stereogenic ligands is limited, especially due to the challenging character of their synthesis.[8-23] Several P-stereogenic ligands have nevertheless been successfully synthesized by alkylation and arylation of phosphine borane complexes. This efficient and promising route consists, first, in the deprotonation of a P-stereogenic secondary phosphine-borane complex and, second, in its C-P phosphination (FIGURE 1).

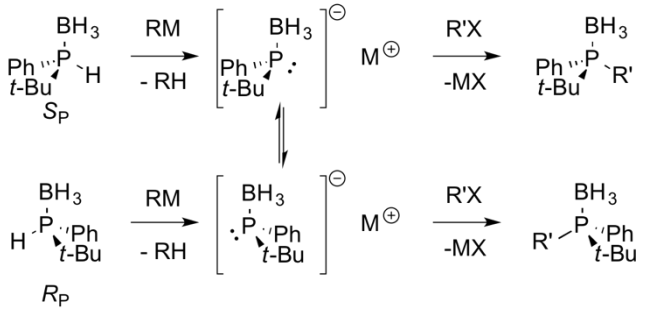

FIGURE 1 Synthesis of P-stereogenic phosphine ligands with lithium *tert*-butylphenylphosphido-borane as intermediate (M = Li).

This synthesis can be made stereoselective using two different methods. The first one uses enantiopure secondary phosphine-borane complexes as starting materials and prevents the racemization of secondary lithium phosphido-borane intermediates.[24-28] On the contrary, the second method uses racemic mixtures as starting materials and resolution is achieved using either a dynamic-thermodynamic[29-31] or a dynamic-kinetic[32-34] strategy. In that case, chirality is induced by a chiral additive that acts stoechiometrically[29-31] and/or catalytically.[32-34] In all cases the efficiency of the chosen method directly depends on the racemization rate of the secondary lithium phosphido-borane intermediate (FIGURE 1).

We here report a joined theoretical and experimental kinetic study of the racemization mechanism of lithium *tert*-butylphenylphosphido-borane. This study aims to improve our understanding of the general racemization mechanism of the secondary lithium phosphido-borane intermediate, which knowledge is subsequently expected to open access to a better control of the asymmetric synthesis of tertiary P-stereogenic phosphines from secondary phosphine-borane complexes.

Materials and Methods

We here postulate a mechanism that possibly involves two parallel reactive routes, a and b (FIGURE 2), which both consist in a monomolecular inversion of the P-stereogenic center, but in which the phosphido-borane entity is either free (route a), or part of a neutral phosphido-borane-lithium solvate (route b). Both routes are additionally connected through two enantiomeric ionic association-dissociation equilibria with $Li^+(THF)_2$ cation.
For this mechanism, reaction and transition standard molar Gibbs free energies $\Delta_rG^{\circ}{}_d$ (dissociation), $\Delta_rG^{\circ\neq}{}_a$ (route a) and $\Delta_rG^{\circ\neq}{}_b$ (route b) are predicted using Density Functional Theory (TABLE 1). Technically, first solvation shells of lithium cations are here explicitly introduced. Free lithium cations consequently come with four explicit tetrahydrofuran molecules, whereas

[a] *Dr. R. Fortrie, Dr. D. Hérault, Dr. A. Béal, Dr. L. Giordano, Prof. G ; Buono*
Aix Marseille Univ, CNRS, Centrale Marseille, iSm2, Marseille, France
E-mail: remy.fortrie@centrale-marseille.fr, gerard.buono@centrale-marseille.fr

[b] *Dr. G. Gatineau*
Univ Grenoble Alpes, CNRS, DCM
UMR5250, BP 53, 38041 Grenoble Cedex 9, France

[c] *Dr. J.-V. Naubron*
Aix Marseille Univ, CNRS, Centrale Marseille, Spectropole-FR1739, Marseille, France

lithium cations that are already bounded to phosphido-borane entities only come with two of them.[35-36]

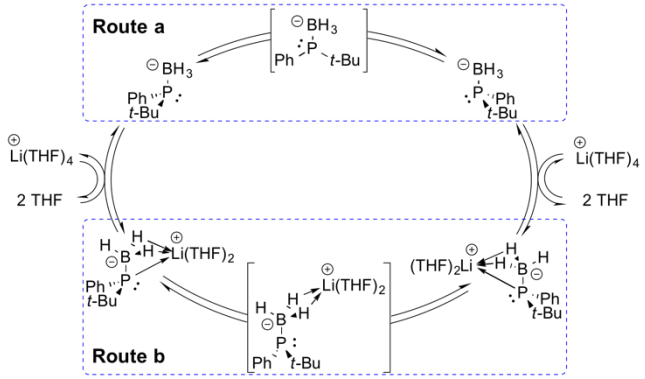

FIGURE 2 Postulated inversion mechanism of lithium *tert*-butylphenylphosphido-borane.

Pyramidal tri-coordinated phosphorous centers are known to invert through either Y-shaped (vertex) or T-shaped (edge) transition structures,[37-39] and both possibilities have consequently been investigated, but only two vertex transition structures have been successfully obtained (FIGURE 3).

TABLE 1 Reaction and transition Gibbs free energies at -20 °C (kJ.mol^{-1}).

	Dissociation (with $Li^+(THF)_2$) $\Delta_rG°_d$	Route a $\Delta_rG°^{\neq}_a$	Route b $\Delta_rG°^{\neq}_b$
Vacuum			
a. B3LYP/6-31+G(d,p)	272.7	69.5	83.7
b. B3LYP/6-31++G**	268.5	70.8	83.2
c. M05-2X/6-31++G**	260.6	84.7	84.7
Vacuum + singlepoint implicit solvent correction			
a//CPCM	36.3	73.7	80.1
c//SMD (6-31G*)	-22.0	89.5	81.2
c//SMD	-9.8	88.7	80.6
Experimental			
See SI §4 for the detailed calculations	8.1	90.2	81.0

The highest occupied molecular orbitals of both transition structures correspond to the lone pair of the phosphorous atom. Interestingly, it appears to be conjugated with all three surrounding groups in an anti-bonding, and then destabilizing, manner, which justifies the existence or the inversion barrier. This effect is however fortunately counterbalanced by the strong inductive effect of the borane group. Without this last influence, the inversion barrier would be much larger, like what is encountered for tertiary phosphines for example.[40-41]

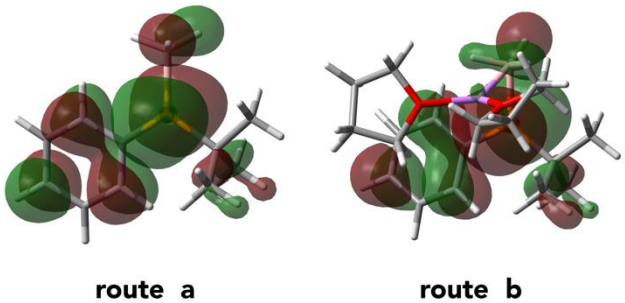

FIGURE 3 Highest occupied molecular orbitals associated to the transition structures encountered along route a and b. Isovalue: 0.02. Calculation level: B3LYP/6-31+G(d,p).

On the right side of FIGURE 3, it can also be seen that the lithium cation is simultaneously bonded to the phosphido-borane anion through the lone pair of the phosphorous atom, and through borane hydrides. This bridged situation forces the borane group to tilt slightly in direction of the lithium cation, and to turn by 30 deg around the PB bond so to make two hydrides simultaneously available for the lithium cation. Electronically, the lithium cation slightly throws the electronic density to itself, but no real dramatic change in formal atomic charge is observed. This lack of drastic difference explains why inversion barriers are similar along routes a and b.

In parallel of the DFT prediction, we attempt to validate the proposed mechanism by measuring $\Delta_rG°_d$ (dissociation), $\Delta_rG°^{\neq}_a$ (route a) and $\Delta_rG°^{\neq}_b$ (route b) by extraction of experimental data. First, for the proposed mechanism to be formally considered as realistic, the measured values must be physically relevant and associated with small uncertainties. Second, for the proposed reaction intermediates and transition structures to be considered as realistic too, measured values must be close enough to their calculated equivalents.

Racemization rates (K_i) of *tert*-butylphenylphosphido-borane have therefore been measured at various temperatures (T_i), for different phosphido-borane concentrations (C_i), and using various durations (t_i) (TABLE 2).

TABLE 2 Racemization rates of lithium *tert*-butylphenylphosphido-borane. Initial enantiomeric excess (ee): 96.0 %.

i	Ti (°C) ±1.5	t_i (min) ±2	C_i (10^{-2} mol.L^{-1})	ee_i (%) ±0.1	K_i (10^{-4} s^{-1})
1	-25.0	60	2.49 ± 0.08	86.4	0.293 ± 0.004
2	-25.0	120	2.77 ± 0.09	63.4	0.577 ± 0.006
3	-25.0	240	2.49 ± 0.08	42.8	0.561 ± 0.003
4	-20.0	60	2.50 ± 0.08	65.9	1.045 ± 0.028
5	-20.0	120	2.67 ± 0.08	48.3	0.954 ± 0.012
6	-20.0	240	2.64 ± 0.08	32.1	0.761 ± 0.004
7	-20.0	60	0.91 ± 0.03	79.5	0.524 ± 0.012
8	-20.0	120	0.91 ± 0.03	65.6	0.529 ± 0.006
9	-15.0	60	2.40 ± 0.08	56.9	1.453 ± 0.041
10	-15.0	120	3.16 ± 0.09	27.9	1.716 ± 0.023
11	-15.0	180	3.33 ± 0.10	18.9	1.505 ± 0.011

These raw data have subsequently been treated using the Rice–Ramsperger–Kassel–Marcus (RRKM) theory of chemical reactivity.[42] Within this framework, kinetic constants $k°_a$ and $k°_b$ are related to $\Delta_rG°^{\neq}_a$ and $\Delta_rG°^{\neq}_b$ through Equations 1 and 2, whereas the dissociation equilibrium constant $K°_d$ depends on $\Delta_rG°_d$ through Equation 3.

$$k°_a = k_B\,T \exp(- \Delta_rG°^{\neq}_a / (R\,T)) / h \quad (1)$$

$$k°_b = k_B\,T \exp(- \Delta_rG°^{\neq}_b / (R\,T)) / h \quad (2)$$

$$K°_d = \exp(- \Delta_rG°_d / (R\,T)) \quad (3)$$

In the present case, on account of the complexity of the proposed mechanism, $\Delta_rG°_d$, $\Delta_rG°^{\neq}_a$ and $\Delta_rG°^{\neq}_b$ cannot be straightforwardly extracted from experimental data. We consequently used the following trick.

As a first step, the nature of each involved species is voluntarily disregarded within the reaction scheme (FIGURE 4).

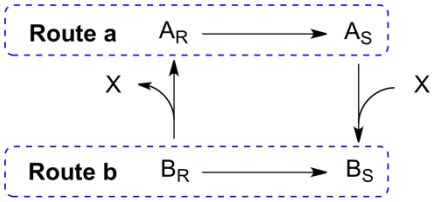

FIGURE 4 Simplified mechanism.

As a second step, based on this simplified mechanism, the expected interdependency between ee, $\Delta_rG°_d$, $\Delta_rG°^{\neq}_a$, $\Delta_rG°^{\neq}_b$, T, C, and t is predicted. This leads to Equation 4, where K(T,C) acts as an overall kinetic constant (Equations 5 and 6).

$$ee(T,C,t) = ee(T,C,0)\ \exp(-K(T,C)\ t) \quad (4)$$

$$K(T,C) = 2\ (\ 2\ k°_a(T) + Q(T,C)\ k°_b(T)\ )\ /\ (\ 2 + Q(T,C)\ ) \quad (5)$$

$$Q(T,C) = (\ 1 + 4\ C\ /\ (\ c°\ K°_d(T)\ )\ )^{1/2} - 1 \quad (6)$$

As a third step, two different sets of global kinetic constants are calculated. The first set, {Ki}, is extracted from measured ee_i and t_i using Equation 7, whereas the second set, {Ki*}, is extracted from measured T_i and C_i using Equation 8, in which $\Delta_rG°_d$, $\Delta_rG°^{\neq}_a$ and $\Delta_rG°^{\neq}_b$ act as parameters.

$$K_i = \ln(\ ee_0\ /\ ee_i\ )\ /\ t_i \quad (7)$$

$$K_i^* = K(\ T_i\ ,\ C_i\ ) \quad (8)$$

The key point here is that, ideally, if the reaction mechanism is realistic, and if the chosen Gibbs free energies are all correct, then {Ki} and {Ki*} sets must be identical.

The last step of the comparison procedure consequently consists in searching for $\Delta_rG°_d$, $\Delta_rG°^{\neq}_a$ and $\Delta_rG°^{\neq}_b$ values that make both {Ki} and {Ki*} sets as close as possible (FIGURE 5). The resulting optimized Gibbs free energies are hereafter referred to as “experimental” (TABLE 1).

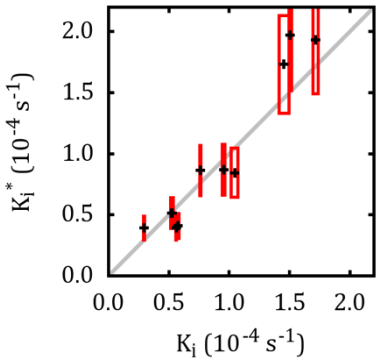

FIGURE 5 Correlation between optimized {Ki} and {Ki*} sets. Red rectangles represent uncertainties.

Technical details

EXPERIMENTAL DETAILS

(*S*)-(+)-*tert*-butylphenylphosphine-borane was prepared from the corresponding secondary phosphine oxide (S_P)-(-)-*tert*-butylphenylphosphine oxide (ee = 99%) according to ref. (25) and (43). The direct ee determination was not possible by chiral HPLC, therefore the derivatization by alkylation was realized, as described below for the racemization study. The starting phosphine-borane is obtained with 96% ee.

Racemization reaction: One equivalent of (*S*)-(+)-*tert*-butylphenyl-phosphine-borane (ee= 96 %) was dissolved at 23 °C in 2 mL of dry THF in a dry Schlenk tube equipped with a magnetic stirrer and an argon inlet. The resulting solution was cooled down to the re-quired temperature with constant stirring and one equivalent of 1.6 M *n*-BuLi in hexanes was added. After the required duration, the reaction was quenched through cooling (−78 °C) and stopped by adding 5 equivalents of benzylbromide. After 30 min, 2 mL of water was added, and the mixture was warmed up to room temperature. It was subsequently extracted 3 times with Et_2O (5 mL), and the combined organic extracts were dried over an-hydrous $MgSO_4$, filtered through silica, and evaporated to dryness. Benzyl-*tert*-butylphenylphosphine-borane was then immediately analyzed using chiral HPLC; Chiralcel OD-3 column; UV detector: 254 nm; flow rate 1 mL.min^{-1}; eluent: hexane/*i*-PrOH 95/5; (*R*)-(+)-benzyl-*tert*-butylphenylphosphine-borane: Rt = 9.37 min; (*S*)-(−)-benzyl-*tert*-butylphenylphosphine-borane: Rt = 11.00 min; k1(+) = 2.12; k2(−) = 2.67, α = 1.26.[44]

THEORETICAL DETAILS

Software: Gaussian03.[45] Optimization and vibrational analysis: gas phase. Solvent correction: singlepoint, solvent=THF. For CPCM: alpha=1.4, tesserae=0.2. Thermodynamics: harmonic oscillator and rigid rotator approximations (including dynamic symmetry factors), solute standard state = infinitely diluted at 1 mol.L^{-1}, solvent standard state = pure liquid.

Results and Discussion

FIGURE 5 shows that the differences between {Ki} and {Ki*} sets are smaller than the rather small uncertainties associated to these sets, which is a first good clue that the proposed mechanism is relevant. Additionally, experimental Gibbs free energies are physically relevant, i.e. reasonable for all, and positive for $\Delta_rG°^{\neq}_a$ and $\Delta_rG°^{\neq}_b$, which is a second good clue that the proposed mechanism is relevant. Moreover, despite the fact that, within the framework of the simplified mechanism, different scenarios can take place depending on $\Delta_rG°_d$, $\Delta_rG°^{\neq}_a$ and $\Delta_rG°^{\neq}_b$ respective values (see supporting information), the scenario that actually comes out exhibits characteristics that are similar to those of the mechanism that has been predicted from DFT calculations: $\Delta_rG°_d$ of a few kJ.mol^{-1} (exp:+8, DFT:-22~36) and a difference of a few kJ.mol^{-1} between $\Delta_rG°^{\neq}_a$ and $\Delta_rG°^{\neq}_b$ (exp:+9, DFT:-6~+8). In other words, all these observations support the proposed racemization mechanism.

This formal agreement comes with a very good numerical concordance for $\Delta_rG°^{\neq}_b$. Indeed, for this value, the deviation between prediction and experiment is within experimental uncertainty (see supporting information). Interestingly, route b experimentally concentrates between 96 % and 99 % of the reaction flow under reaction conditions. In other words, a very good concordance is here obtained for the most significant route of the proposed inversion mechanism.

On another hand, route a, the minor reactive route, only represents between 1 % and 4 % of the total reaction flow. This implies an extremely large experimental uncertainty for the $\Delta_rG°^{\neq}_a$ value, and no definitive conclusion can consequently be drawn in this case.

Finally, the experimental value obtained for $\Delta_rG°_d$ confirms the existence of an association-dissociation equilibrium that plays a significant role in the inversion mechanism. The deviation obtained in this case between prediction and experiment is however outside the experimental uncertainty area (see supporting information). This suggests that either not all species involved in this equilibrium have been taken into account within DFT calculations, and/or that the chosen in silico methodology is not suitable for the association/dissociation reaction. This issue is however not critical for the present study and could be addressed in the future.

Conclusion

As a conclusion, we here investigated both theoretically and experimentally the racemization kinetic of lithium *tert*-butylphenylphosphido-borane in THF solution. Practically, this

process consisted in testing the validity of DFT predictions by fitting experimental data with a simplified version of the proposed mechanism. Based on this approach, the following inversion mechanism can confidently be proposed. The inversion consists in an association-dissociation equilibrium, which significance had not yet been estimated in previous papers, in which the associated form, a [phosphido-borane-Li(THF)$_2$] neutral solvate, inverts monomolecularly via a vertex transition structure ($\Delta_r G^{\circ\neq}$: 81 kJ.mol^{-1}). For comparison with our study, an inversion barrier of 140 kJ.mol^{-1} has been experimentally evaluated for the lithium *tert*-butylmethylphosphidoborane.[46] This example illustrates the importance of the substituent bound to the phosphorus atom on the inversion barrier. The phenyl substituent, as expected, stabilizes the transition state due to the enabled delocalization of the lone pair. Moreover, the nature of metal cation can be a key parameter for the ion pairing with the phosphido-borane, for which the configurational stability could be affected.[47] Further studies will evaluate the interdependency between the substituents bounded to the stereogenic phosphorous center and the transition Gibbs free energy associated to the inversion step.

Acknowledgements

AB, JVN and RF thank the Centre Régional de Compétences en Modélisation Moléculaire (CRCMM) and the Centre Informatique National de l'Enseignement Supérieur (CINES) for computational ressources. DG thanks the Ministère de l'Enseignement Supérieur et de la Recherche for funding support.

Data availability statement

The data that support the findings of this study are available from the corresponding author upon reasonable request.

Supporting information

Full experimental data, kinetic models, fitting procedures, DFT and thermodynamic data may be found as supporting information in the online version of this article at the publisher's website.

REFERENCES AND NOTES

(1) Kamer PCJ, van Leeuwen PWNM. *Phosphorus(III) Ligands in Homogeneous Catalysis: Design and Synthesis.* John Wiley & Sons Ltd., **2012**.
(2) Zhou, QL *Privileged Chiral Ligands and Catalysts*. Wiley-VCH: Weinheim, **2011.**
(3) Börner A. *Phosphorus Ligands in Asymmetric Catalysis; Synthesis and Applications.* Wiley-VCH Verlag GmbH & Co. KGaA, **2008**.
(4) Lühr S, Holz J, Börner A. The Synthesis of Chiral Phosphorus Ligands for Use in Homogeneous Metal Catalysis. *ChemCatChem* **2011**;3:1708-1730.
(5) Marinetti A, Voituriez A. Enantioselective Phosphine Organocatalysis. *Synlett* **2010**:174-194.
(6) Gomez C, Betzer J-F, Voituriez A, Marinetti A. Phosphine Organocatalysis in the Synthesis of Natural Products and Bioactive Compounds. *ChemCatChem* **2013**;5:1055-1065.
(7) Benaglia M, Rossi S. Chiral Phosphine Oxides in Present-Day Organocatalysis. *Org Biomol Chem* **2010**;8:3824-3830.
(8) Grabulosa A. *P-Stereogenic Ligands in Enantioselective Catalysis.* Royal Society of Chemistry Publishing, **2011**.
(9) Lemouzy S, Giordano L, Hérault D, Buono G. Introducing Chirality at Phosphorus Atoms: An Update on the Recent Synthetic Strategies for the Preparation of Optically Pure P-Stereogenic Molecules: Introducing Chirality at Phosphorus Atoms: An Update on the Recent Synthetic Strategies for the Preparation of Optically Pure P-Stereogenic Molecules. *Eur J Org Chem* **2020**;23:3351-3366.
(10) Han ZS, Goyal N, Herbage MA, Sieber JD, Qu B, Xu Y, Li Z, Reeves JT, Desrosiers J-N, Ma S, Grinberg N, Lee H, Mangunuru HPR, Zhang Y, Krishnamurthy D, Lu BZ, Song JJ, Wang G, Senanayake CH. Efficient Asymmetric Synthesis of *P* -Chiral Phosphine Oxides via Properly Designed and Activated Benzoxazaphosphinine-2-Oxide Agents. *J Am Chem Soc* **2013**;135:2474-2477.
(11) Casimiro M, Roces L, García-Granda S, Iglesias MJ, López Ortiz F. Directed *Ortho* -Lithiation of Aminophosphazenes: An Efficient Route to the Stereoselective Synthesis of *P* -Chiral Compounds. *Org Lett* **2013**;15:2378-2381.
(12) Berger O, Montchamp J-L. A General Strategy for the Synthesis of P-Stereogenic Compounds. *Angew Chem Int Ed* **2013**;52:11377-11380. (f) Zijlstra H, León T, de Cózar A, Guerra CF, Byrom D, Riera A, Verdaguer X, Bickelhaupt FM. Stereodivergent SN2@P Reactions of Borane Oxazaphospholidines: Experimental and Theoretical Studies. *J Am Chem Soc* **2013**;135:4483-4491.
(13) Mohar B, Čusak A, Modec B, Stephan M. *P* -Stereogenic Phospholanes or Phosphorinanes from *o* -Biarylphosphines: Two Bridges Not Too Far. *J Org Chem* **2013**;78:4665-4673.
(14) Ding B, Zhang Z, Xu Y, Liu Y, Sugiya M, Imamoto T, Zhang W. P-Stereogenic PCP Pincer–Pd Complexes: Synthesis and Application in Asymmetric Addition of Diarylphosphines to Nitroalkenes. *Org Lett* **2013**;15:5476-5479.
(15) Nikitin K, Rajendran KV, Müller-Bunz H, Gilheany DG. Turning Regioselectivity into Stereoselectivity: Efficient Dual Resolution of P-Stereogenic Phosphine Oxides through Bifurcation of the Reaction Pathway of a Common Intermediate. *Angew Chem Int Ed* **2014**;53:1906-1909.
(16) Adams H, Collins RC, Jones S, Warner CJA. Enantioselective Preparation of P-Chiral Phosphine Oxides. *Org Lett* **2011**;13:6576-6579.
(17) Granander J, Secci F, Canipa SJ, O'Brien P, Kelly B. One-Ligand Catalytic Asymmetric Deprotonation of a Phosphine Borane: Synthesis of P-Stereogenic Bisphosphine Ligands. *J Org Chem* **2011**;76:4794-4799.
(18) Takizawa S, Rémond E, Arteaga FA, Yoshida Y, Sridharan V, Bayardon J, Jugé S, Sasai H. P-Chirogenic Organocatalysts: Application to the Aza-Morita–Baylis–Hillman (Aza-MBH) Reaction of Ketimines. *Chem Commun* **2013**;49:8392-8394.
(19) Kortmann FA, Chang M-C, Otten E, Couzijn EPA, Lutz M, Minnaard AJ. Consecutive Dynamic Resolutions of Phosphine Oxides. *Chem Sci* **2014**;5:1322-1328.

(20) Harvey JS, Gouverneur V. Catalytic Enantioselective Synthesis of P-Stereogenic Compounds. *Chem Commun* **2010**;46:7477-7485.
(21) Glueck DS. Catalytic Asymmetric Synthesis of Chiral Phosphanes. *Chem Eur J* **2008**;14:7108-7117.
(22) Glueck DS, Metal-Catalyzed Asymmetric Synthesis of P-Stereogenic Phosphines. *Synlett* **2007**:2627-2634.
(23) Glueck DS. Catalytic Asymmetric Synthesis of P-Stereogenic Phosphines: Beyond Precious Metals. *Synlett* **2021**;31:875-884.
(24) Stankevič M, Pietrusiewicz KM. Resolution and Stereochemistry of *Tert* -Butylphenylphosphinous Acid−Borane. *J Org Chem* **2007**;72:816-822.
(25) Gatineau D, Giordano L, Buono G. Bulky, Optically Active P-Stereogenic Phosphine–Boranes from Pure H-Menthylphosphinates. *J Am Chem Soc* **2011**;133:10728-10731.
(26) Imamoto T, Tamura K, Zhang Z, Horiuchi Y, Sugiya M, Yoshida K, Yanagisawa A, Gridnev ID. Rigid P-Chiral Phosphine Ligands with *Tert*-Butylmethylphosphino Groups for Rhodium-Catalyzed Asymmetric Hydrogenation of Functionalized Alkenes. *J Am Chem Soc* **2012**;134:1754-1769.
(27) Rémond E, Bayardon J, Takizawa S, Rousselin Y, Sasai H, Jugé S. O-(Hydroxyalkyl)Phenyl P-Chirogenic Phosphines as Functional Chiral Lewis Bases. *Org Lett* **2013**;15:1870-1873.
(28) Recently a highly enantioselective catalytic synthesis of P-stereogenic secondary phosphine borane followed by P-C formation with alkyl halides have been reported Wang C, Huang K, Ye J, Duan W-L. Asymmetric Synthesis of P-Stereogenic Secondary Phosphine-Boranes by an Unsymmetric Bisphosphine Pincer-Nickel Complex. *J Am Chem Soc* **2021**;143:5685-5690.
(29) Wolfe B, Livinghouse T. A Direct Synthesis of P-Chiral Phosphine-Boranes via Dynamic Resolution of Lithiated Racemic *Tert*-Butylphenylphosphine-Borane with (-)-Sparteine. *J Am Chem Soc* **1998**;120:5116-5117.
(30) Heath H, Wolfe B, Livinghouse T, Bae SK. New Methods for the Synthesis of P-Chirogenic Diphosphines: An Application to the Development of an Improved Asymmetric Variation of the Rh(I)-Catalyzed [4 + 2] Cycloaddition. *Synthesis* **2001**:2341-2347.
(31) Headley CE, Marsden SP. Synthesis and Application of *P* -Stereogenic Phosphines as Superior Reagents in the Asymmetric Aza-Wittig Reaction. *J Org Chem* **2007**;72:7185-7189.
(32) Moncarz JR, Brunker TJ, Glueck DS, Sommer RD, Rheingold AL, *J Am Chem Soc* **2003;**125: 1180-1181. (b) Pican S, Gaumont A-C. Palladium Catalysed Enantioselective Phosphination Reactions Using Secondary Phosphine-Boranes and Aryl Iodide. *Chem Commun* **2005**:2393-2395.
(33) Huang Y, Li Y, Leung P-H, Hayashi T. Asymmetric Synthesis of *P* -Stereogenic Diarylphosphinites by Palladium-Catalyzed Enantioselective Addition of Diarylphosphines to Benzoquinones. *J Am Chem Soc* **2014**;136:4865-4868.
(34) Chan VS, Chiu M, Bergman RG, Toste FD. Development of Ruthenium Catalysts for the Enantioselective Synthesis of P-Stereogenic Phosphines via Nucleophilic Phosphido Intermediates. *J Am Chem Soc* **2009**;131:6021-6032.
(35) Pratt LM, Truhlar DG, Cramer CJ, Kass SR, Thompson JD, Xidos JD. Aggregation of Alkyllithiums in Tetrahydrofuran. *J Org Chem* **2007**;72:2962-2966.
(36) Barozzino Consiglio G, Queval P, Harrison-Marchand A, Mordini A, Lohier J-F, Delacroix O, Gaumont A-C, Gérard H, Maddaluno J, Oulyadi H. $Ph_2P(BH_3)Li$: From Ditopicity to Dual Reactivity. *J Am Chem Soc* **2011**;133:6472-6480.
(37) Dixon DA, Arduengo AJ. Periodic Trends in the Edge and Vertex Inversion Barriers for Tricoordinate Pnicogen Hydrides and Fluorides. *J Am Chem Soc* **1987**;109:338-341.
(38) Toselli N, Fortrie R, Martin D, Buono G. New P-Stereogenic Triaminophosphines and Their Derivatives: Synthesis, Structure, Conformational Study, and Application as Chiral Ligands. *Tetrahedron: Asymmetry* **2010**;21:1238-1245.
(39) Izod K, Clark ER, Stewart J. Edge- versus Vertex-Inversion at Trigonal Pyramidal Ge(II) Centers—A New Aromatic Anchimerically Assisted Edge-Inversion Mechanism. *Inorg Chem* **2011**;50:3651-3661.
(40) Baechler RD, Mislow K. Effect of Structure on the Rate of Pyramidal Inversion of Acyclic Phosphines. *J Am Chem Soc* **1970**;92:3090-3093.
(41) For a catalyzed pyramidal inversion see: Reichl KD, Ess DH, Radosevich AT. Catalyzing Pyramidal Inversion: Configurational Lability of P-Stereogenic Phosphines via Single Electron Oxidation. *J Am Chem Soc* **2013**;135:9354-9357.
(42) McNaught AD, Wilkinson A. *IUPAC. Compendium of Chemical Terminology*; 2nd ed. ("The Gold Book"); Blackwell Scientific Publications: Oxford, **1997**.
(43) Leyris A, Bigeault J, Nuel D, Giordano L, Buono G. Enantioselective synthesis of secondary phosphine oxides from (R_P)-(−)-menthyl hydrogenophenylphosphinate. *Tetrahedron Letters* **2007**;48(30):5247-5250.
(44) For complementary experimental details see table S1 in supporting information and ref: 5b for analytical characterization.
(45) *Gaussian 03, Revision C.02,* Frisch, MJ, Trucks, GW, Schlegel, HB, Scuseria, GE, Robb, MA, Cheeseman, JR, Montgomery Jr, JA, Vreven, T, Kudin, KN, Burant, JC, Millam, JM, Iyengar, SS, Tomasi, J, Barone, V, Mennucci, B, Cossi, M, Scalmani, G, Rega, N, Petersson, GA, Nakatsuji, H, Hada, M, Ehara, M, Toyota, K, Fukuda, R, Hasegawa, J, Ishida, M, Nakajima, T, Honda, Y, Kitao, O, Nakai, H, Klene, M, Li, X, Knox, JE, Hratchian, HP, Cross, JB, Bakken, V, Adamo, C, Jaramillo, J, Gomperts, R, Stratmann, RE, Yazyev, O, Austin, AJ, Cammi, R, Pomelli, C, Ochterski, JW, Ayala, PY, Morokuma, K, Voth, GA, Salvador, P, Dannenberg, JJ, Zakrzewski, VG, Dapprich, S, Daniels, AD, Strain, MC, Farkas, O, Malick, DK, Rabuck, AD, Raghavachari, K, Foresman, JB, Ortiz, JV, Cui, Q, Baboul, AG, Clifford, S, Cioslowski, J, Stefanov, BB, Liu, G, Liashenko, A, Piskorz, P, Komaromi, I, Martin, R, Fox, DJ, Keith, T, Al-Laham, MA, Peng, CY, Nanayakkara, A, Challacombe, M, Gill, PMW, Johnson, B, Chen, W, Wong, MW, Gonzalez, C, and Pople, JA, Gaussian, Inc., Wallingford CT, **2004**.
(46) Miura T, Yamada H, Kikuchi S, Imamoto T. Synthesis and Reactions of Optically Active Secondary Dialkylphosphine-Boranes. *J Org Chem* **2000**;65:1877-1880.
(47) For the phosphido-borane complex $[\{(Me_3Si)_2CH\}(Ph)P(BH_3)][Na(12\text{-crown-}4)_2]$ an inversion barrier of 61.1 $kJ.mol^{-1}$ have been determined: Izod K, Watson JM, Clegg W, Harrington RW. Phosphido-Borane and Phosphido-Bis(Borane) Complexes of the Alkali Metals, a Comparative Study. *Inorg Chem* **2013**;52:1466-1475.